Oxygen Reduction on Platinum Low-Index Single-Crystal Surfaces in Sulfuric Acid Solution: Rotating Ring-Pt(hkl) Disk Studies

ARTICLE *in* THE JOURNAL OF PHYSICAL CHEMISTRY · MARCH 1995

Impact Factor: 2.78 · DOI: 10.1021/j100011a001

3 AUTHORS, INCLUDING:

N. M. Marković
Argonne National Laboratory
284 PUBLICATIONS **21,961** CITATIONS
SEE PROFILE

Philip N Ross
University of California, Berkeley
360 PUBLICATIONS **21,364** CITATIONS
SEE PROFILE

The Journal of Physical Chemistry

 VOLUME 99, NUMBER 11, MARCH 16, 1995

LETTERS

Oxygen Reduction on Platinum Low-Index Single-Crystal Surfaces in Sulfuric Acid Solution: Rotating Ring–Pt(*hkl*) Disk Studies

Nenad M. Marković,* Hubert A. Gasteiger, and Philip N. Ross, Jr.

Materials Science Division, Lawrence Berkeley Laboratory, Berkeley, California 94720

Received: September 28, 1994; In Final Form: December 16, 1994[⊗]

The first results of a study of the oxygen reduction reaction on a rotating ring–disk electrode using single-crystal Pt disk electrodes are presented. The order of activity of Pt(*hkl*) in H_2SO_4 increased in the sequence (111) < (100) < (110). These differences are attributed to the structure sensitivity of (bi)sulfate anion adsorption and its inhibiting effect. Very small fluxes ($I_R/N < 0.01I_D$) of peoxide were detected at the ring at potentials above 0 V (SCE) on all surfaces. However, below 0 V adsorbed hydrogen affected the partial reduction of oxygen to H_2O_2 in the order (111) < (100) > (110), with 100% H_2O_2 formation on Pt(111).

1. Introduction

The reduction of oxygen on a platinum electrode is one of the most widely studied electrochemical reactions.[1,2] The early work with polycrystalline electrodes has been followed more recently by work with single-crystal surfaces in order to establish the influence of the surface structure on the mechanism and the kinetics of this reaction. In 1979, Ross reported essentially the same activity for oxygen reduction on all three Pt low-index planes.[3] In his experiments, kinetic oxygen reduction currents were recorded on a stationary electrode by means of measuring in a narrow and very positive potential region, which may have caused partial disorder of the low-index planes by oxide formation. The separation of kinetic and diffusion currents at less positive potentials on platinum single crystals can be achieved with a rotating hanging meniscus electrode (RHME), and Marković *et al.*[4,5] found that the activity for oxygen reduction in 0.1 M $HClO_4$ decreases in the sequence (110) > (111) > (100). Analysis of their RHME data showed that O_2 reduction mainly involves a four-electron reduction to water as the main product, and the kinetics were found to be first order with respect to O_2 on all three low-index surfaces. On the other hand, Kadiri *et al.*,[6] employing the same method, found that O_2 reduction in 1 M $HClO_4$ is essentially insensitive to the Pt surface structure but is structure-sensitive in solutions containing strongly adsorbing anions like (bi)sulfate, phosphate, or Cl^-, indicating that the structure sensitivity arises from structure-sensitive adsorption of anions which impede the reaction. The activity of the platinum single crystals in solutions containing strongly adsorbing anions increased in the order Pt(111) < Pt-(100) < Pt(110).

In spite of substantial efforts directed toward maintaining surface and electrolyte cleanliness while controlling the dynamics of O_2 transport (by utilizing a RHME), experimental difficulties still impede a definitive determination of the effect of the crystallographic orientation of Pt single crystals on the kinetics of O_2 reduction; *e.g.*, contributions from the edge of the single crystal are difficult to avoid. It would be desirable to measure oxygen reduction currents in a true rotating disk electrode (RDE) geometry or even better in a rotating ring–disk electrode (RRDE), the latter of which would allow one to monitor the formation of H_2O_2 on the ring and thereby to precisely assess the effect of surface structure on the reaction mechanism/pathway.[1,2]

* To whom correspondence should be addressed: Lawrence Berkeley Labortory, Mail Stop 2-100, 1 Cyclotron Road, Berkeley, CA 94720. Phone: (510) 486-4793; FAX: (510) 486-5530.

[⊗] Abstract published in *Advance ACS Abstracts,* March 1, 1995.

0022-3654/95/2099-3411$09.00/0

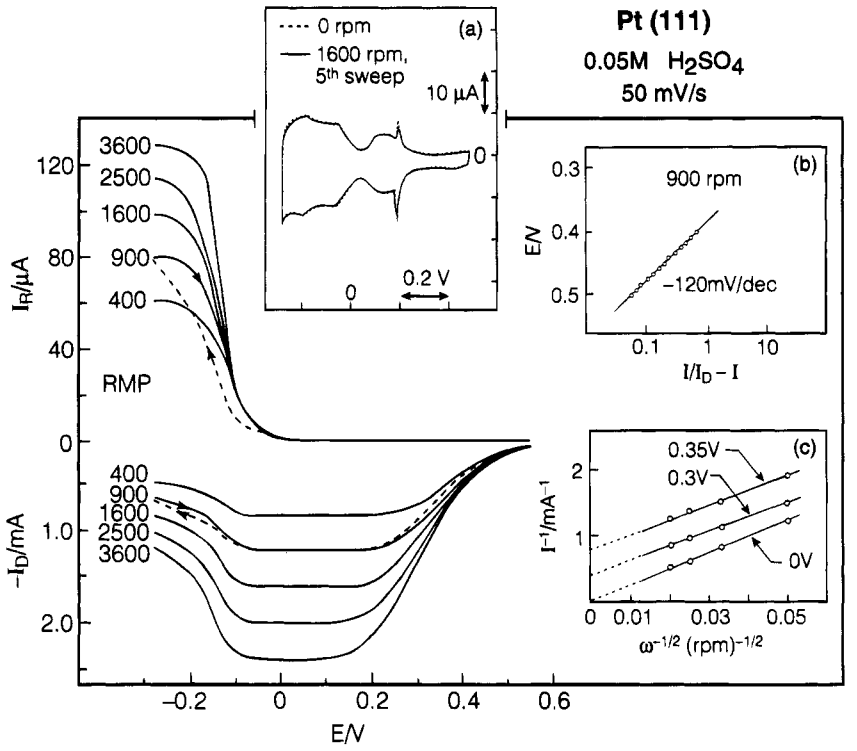

Figure 1. Disk (I_D) and ring (I_R) currents during oxygen reduction on Pt(111) in 0.05 M H_2SO_4 at a sweep rate of 50 mV/s (ring potential = 0.95 V): (—) positive-going sweeps; (- - -) negative-going sweep at 900 rpm. (a) Cyclic voltammetry of Pt(111) in the RRDE assembly in oxygen-free electrolyte with and without rotation. (b) Tafel plot at 900 rpm. (c) Levich plot at various electrode potentials.

The aim of this paper is to report a new experimental method for the fast assembly of rotating ring–platinum single-crystal disk electrodes and to present the first results for the detection of peroxide on the ring electrode during the O_2 reduction on Pt single-crystal disk electrodes. This new type of electrode assembly has allowed us to study the effect of the structure sensitivity of (bi)sulfate anion and hydrogen adsorption on the kinetics and the mechanism of O_2 reduction on Pt(*hkl*); the rotating ring–platinum single-crystal disk electrode can be extended easily to UHV-prepared surfaces[7] and to study underpotential deposition of metals on single-crystal electrodes.[8,9]

2. Experimental Section

Cylindrical single-crystal samples with a diameter of 0.600 cm and length of 0.4 cm were cut by centerless grinding and mounted into a Pine Instruments interchangeable ring–(Pt) disk electrode arbor.[10] The collection efficiency, N, was measured using potassium ferrocyanide; independent measurements on all the low-index single-crystal disk electrodes yielded a value of 0.22 ± 5%, in fairly good agreement with its theoretical value of 0.24[11] based on the design dimensions of the ring–disk electrode. Following flame annealing and cooling in H_2, with the surface protected by a drop of pure water,[12] the crystal was placed face down on a polypropylene film covered with a thin film of water. (Our previous X-ray scattering experiments showed that single-crystal platinum electrodes protected with the water and covered with a polypropylene film remained clean for several hours.[13]) After the careful removal of residual water from the edge of the crystal, the cylindrical samples were pressed into the disk position in the arbor. Subsequently, the polypropylene film was removed, and before the transfer of the rotating arbor into the electrochemical cell, a drop of pure water was placed onto the single crystal. The electrode was immersed into the 0.05 M H_2SO_4 electrolyte (Baker Ultrex, prepared with pyrolytically triply distilled water) under potential control at 0.2 V vs SCE; oxygen (Air Products, 5N8 purity) was bubbled through a glass frit. The ring was potentiostated at 0.95 V, where peroxide oxidation (Merck Suprapure) occurred under diffusion control. The geometrical surface area of the disk electrodes was 0.283 cm^2, and all voltammograms were recorded with a sweep rate of 50 mV/s at 25 °C, with potentials being referenced to the saturated calomel electrode (SCE). A bridge was placed between the reference electrode and the cell, preventing electrolyte contamination by Cl^-.

3. Results and Discussion

The validity of the crystal preparation and the clean assembling of the rotating ring–disk electrode was verified by the voltammetry recorded on platinum single-crystal electrodes mounted in the ring–disk electrode assembly (inserts a of Figures 1–3). Cyclic voltammograms in oxygen-free 0.05 M H_2SO_4 of all three electrodes are characteristic for well-oriented and clean low-index platinum single crystals, confirming that the flame-annealed Pt(*hkl*) crystals remained clean during the mounting procedure. Even more importantly, the cyclic voltammograms of Pt(*hkl*) electrodes recorded at 1600 rmp were essentially identical with the ones obtained under stationary conditions (inserts a in Figures 1–3), implying that both electrode assembly and the solution were extremely clean. Considering the strong inhibiting effect of impurities on O_2 reduction kinetics,[1] this marks an important development which allowed us, *for the first time*, to employ the RRDE technique in the study of oxygen reduction on platinum single crystals.

Figures 1–3 show ring–disk measurements on platinum low-index single crystals in O_2-saturated 0.05 M H_2SO_4. On all three single-crystal electrodes, following a potential region where there is mixed kinetic–diffusion control of the reaction, well-defined diffusion limiting currents were recorded over a wide potential region. In both potential regions, the ring currents on Pt(*hkl*) surfaces were a very small fraction of the disk currents (*i.e.*, $I_R/N < 0.01 I_D$), implying that oxygen reduction proceeds

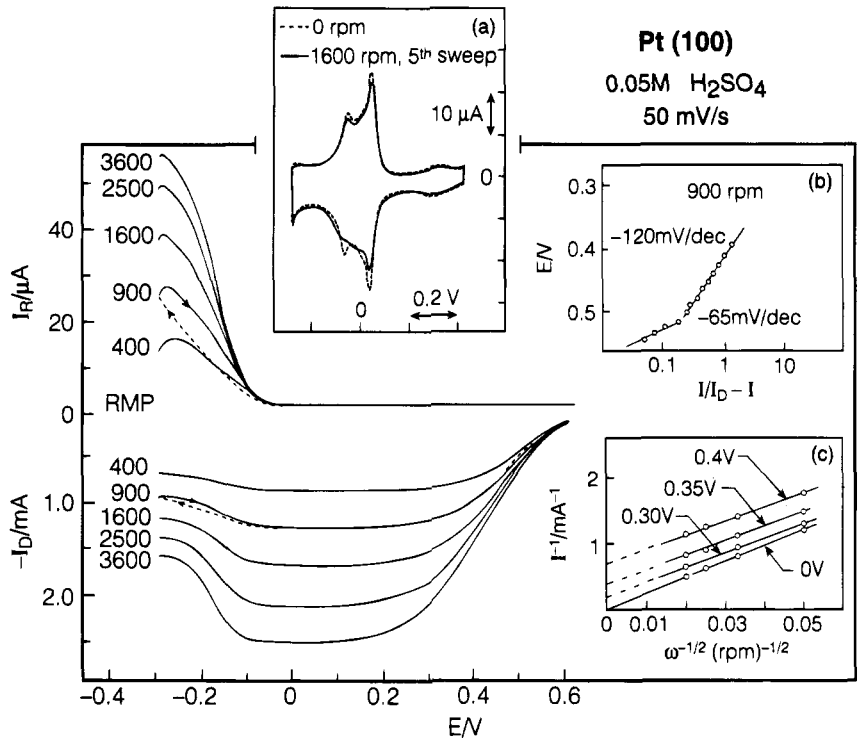

Figure 2. Disk (I_D) and ring (I_R) currents during oxygen reduction on Pt(100) in 0.05 M H_2SO_4 at a sweep rate of 50 mV/s (ring potential = 0.95 V): (—) positive-going sweeps; (- - -) negative-going sweep at 900 rpm. (a) Cyclic voltammetry of Pt(100) in the RRDE assembly in oxygen-free electrolyte with and without rotation. (b) Tafel plot at 900 rpm. (c) Levich plot at various electrode potentials.

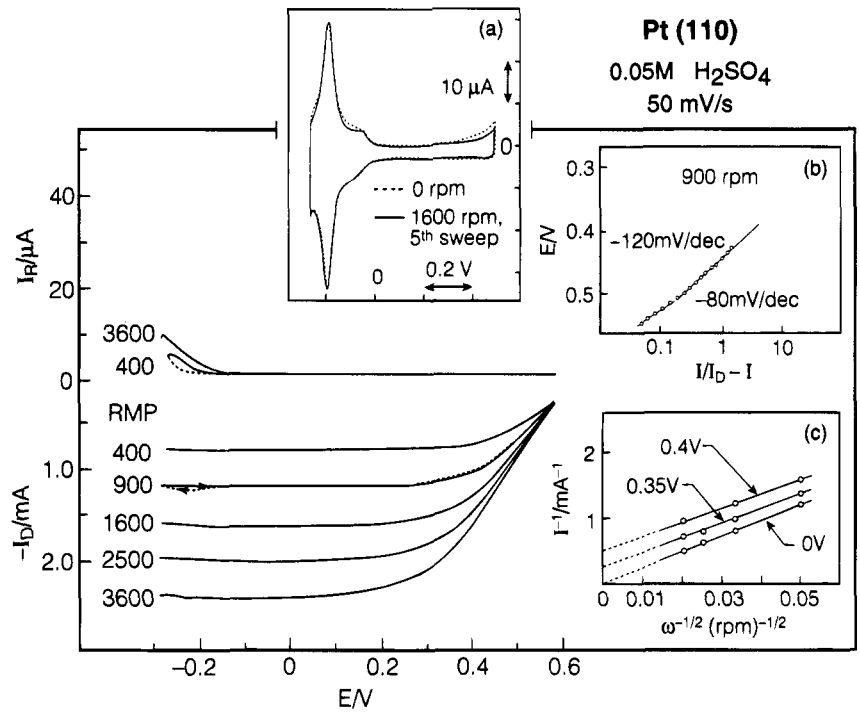

Figure 3. Disk (I_D) and ring (I_R) currents during oxygen reduction on Pt(110) in 0.05 M H_2SO_4 at a sweep rate of 50 mV/s (ring potential = 0.95 V): (—) positive-going sweeps; (- - -) negative-going sweep at 900 rpm. (a) Cyclic voltammetry of Pt(110) in the RRDE assembly in oxygen-free electrolyte with and without rotation. (b) Tafel plot at 900 rpm. (c) Levich plot at various electrode potentials.

almost entirely through the direct four-electron pathway. At *ca.* −0.1 V, however, the activity for O_2 reduction on Pt(111) (see Figure 1) starts to decrease, at −0.25 V reaching half of the value of the diffusion-limiting current for the four-electron process. A similar behavior was observed on Pt(100) (see Figure 2), although the decrease in the disk current is smaller than for Pt(111). This change in O_2 reduction currents is accompanied quantitatively by the appearance of H_2O_2 oxidation currents on the ring electrode (*i.e*, $\Delta I_D = 2I_R/N$). Comparison with the voltammetry in O_2-free electrolyte indicates that the onset of peroxide formation coincides with the potential for the onset of hydrogen adsorption on these two surfaces. Quite different behavior is observed on Pt(110), Figure 3, where the ring currents for peroxide oxidation below −0.1 V were almost invisible.

An analysis of the disk currents shows that the O_2 reduction on all single crystals is first order with respect to dissolved O_2 (inserts c in Figures 1−3). A plot of I^{-1} vs $\omega^{-0.5}$ for various

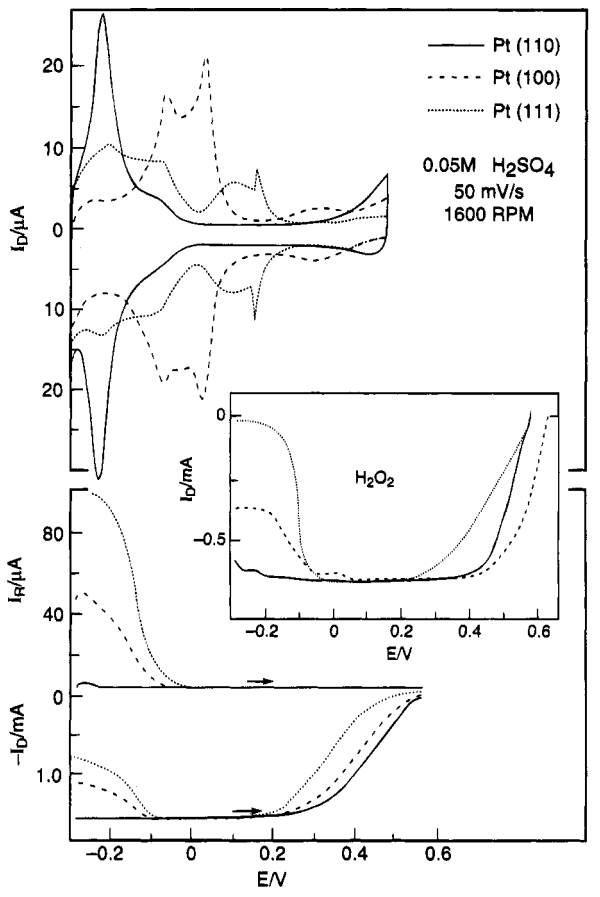

Figure 4. Top: cyclic voltammetry of Pt(*hkl*) in oxygen-free electrolyte in the RRDE assembly (fifth sweep). Bottom: disk (I_D) and ring (I_R) currents during oxygen reduction on Pt(*hkl*) (ring potential = 0.95 V). Insert: reduction of 1.2 × 10^{-3} M H_2O_2 on Pt(*hkl*) mounted in the RRDE assembly (0.05 M H_2SO_4, 50 mV/s, 1600 rpm).

potentials yields straight lines with intercepts corresponding to the kinetic currents, I_k (note that I_k (110) > I_k(100) > I_k(111)); their slope, the so-called *B* factor, allows one to assess the number of electrons involved in the oxygen reduction reaction. The experimental value of *B*, 4.24 × 10^{-2} mA $rpm^{-0.5}$, evaluated from Figures 1−3 agrees well with the theoretical value, 4.27 × 10^{-2} mA $rpm^{-0.5}$, for a four-electron reduction using literature data for O_2 solubility (1.26 × 10^{-3} mol/L[14,15]), viscosity (1.009 × 10^{-2} cm^2/s[14]), and oxygen diffusivity (1.93 × 10^{-5} cm^2/s in 0.1 M $HClO_4$ with very similar viscosity[16]). The simplest and the most logical explanation for the higher overpotential for O_2 reduction on the Pt(111) surface (see Figure 4) is that its activity is reduced by the relatively strong adsorption of tetrahedrally bonded (bi)sulfate anions on the (111) sites observed in recent FTIR[17] and radiotracer experiments,[18] both of which report the onset of (bi)sulfate adsorption at ≈0.15 V, the same potential at which the onset of kinetic currents can be observed on Pt(111), Figures 1 and 4. The absolute magnitude of (bi)sulfate coverage derived from radiotracer experiments on Pt(111) in 1 mM H_2SO_4 is *ca.* 0.2 monolayer, which is a factor of 2−3 higher than on Pt(100).[19] Furthermore, from FTIR experiments it has emerged that (bi)sulfate adsorption on Pt(111) is significantly stronger than on Pt(100)[20] and that the bonding of (bi)sulfate to the Pt(111) surface is through all three equivalent oxygen atoms, in contrast to (bi)sulfate adsorption on Pt(100) and Pt(110) where only one or two oxygen atoms are bonded to the surface resulting in a reduced adsorption strength.[20,21] These differences of (bi)sulfate adsorption in terms of coverage and bonding between Pt(111) and the other two low-index faces are consistent with the significantly lower activity of Pt(111) for oxygen reduction compared to either Pt(100) or Pt(110) (Figure 4). The most active surface for oxygen reduction is the Pt(110) plane, as was also found for O_2 reduction in 0.1 M $HClO_4$.[4,5,22] The difference in activity between Pt(110) and Pt(100) in sulfuric acid electrolyte may derive either from subtle differences in (bi)sulfate adsorption or from other structure-sensitive surface processes, such as the adsorption of oxygen-containing species. The fact that the activity of all three low-index platinum planes is significantly higher in $HClO_4$[22] does, however, suggest that the major differences in H_2SO_4 electrolyte stem from the structure-sensitive adsorption of (bi)sulfate anions. It should be pointed out that although (bi)sulfate adsorption onto the Pt(*hkl*) surface inhibits the reduction of molecular O_2, probably by blocking the initial adsorption of O_2, it does *not* affect the pathway of the reaction since no H_2O_2 is detected on the ring electrode for any of the surfaces in the kinetically controlled potential region.

The inserts b of Figures 1−3 show Tafel plots for Pt(*hkl*) surfaces. Pt(111) has a 120 mV dec^{-1} Tafel slope in the entire potential region. Pt(100) and Pt(110), however, have two Tafel slopes as is usually observed on polycrystalline platinum,[1] faceted,[23] and single-crystal surfaces,[5,6] *i.e.*, 60 mV dec^{-1} at low currents and 120 mV dec^{-1} at high currents. The transition in the Tafel slope on both Pt(100) and Pt(110) is probably related to the onset of the adsorption of oxygen-containing species, OH_{ads}, and to the effect these spectator species have on the adsorption of O_2 from the solution phase. The differing potentials for the onset of OH_{ads} formation on the Pt(*hkl*) surfaces are easily seen in the voltammetry curves in oxygen-free electrolyte in Figure 4. On Pt(100) and Pt(110), OH_{ads} formation initiates at ≈0.4−0.5 V, but on Pt(111) it does not occur before ≈0.8 V.[24,25] Thus, the absence of a transition in the Tafel slope on Pt(111) anywhere in the potential region where oxygen reduction is observed (Figure 1) is consistent with all of these concepts for surface processes on Pt.

Figure 4 also shows that the oxygen reduction reaction is very structure sensitive in the hydrogen adsorption region (≲0 V). This observation is not new and was reported earlier by Marković *et al.*[4,5] The important new results is that the amount of H_2O_2 produced on the disk was simultaneously monitored on the ring electrode. The activity for oxygen reduction on the H_{ads}-modified electrodes decreases in the order Pt(110) > Pt(100) > Pt(111), and the decrease in disk currents is followed *quantitatively* by an increase in the ring currents measuring the flux of peroxide; the limiting current on Pt(111) thus corresponds to an exactly two-electron reduction of O_2 at the negative potential limit. This implies that the change in the mechanism/pathway of oxygen reduction in the hydrogen adsorption region is most likely related with peroxide formation: hydrogen on Pt(111), and to a lesser extent on Pt(100), seems to decrease the number of sites which are available for breaking the O−O bond necessary for the four-electron reduction pathway. The ring−disk results in Figure 4 indicate that peroxide intermediate formed on the Pt(111) disk electrode (to a lesser extent on Pt(100)) is neither chemically decomposed nor further electrochemically reduced in this potential region. We sought to confirm this conclusion independently by examining the reduction of hydrogen peroxide on the Pt(*hkl*) disk electrodes in oxygen-free electrolyte. To simulate the chemical environment during O_2 reduction, we added peroxide to the supporting electrolyte to a concentration approximating the level of peroxide produced during the oxygen reduction, *i.e.*, equal to the solubility concentration of oxygen in the electrolyte. The insert of Figure 4 shows the peroxide reduction currents obtained on the three platinum low-index surfaces. As expected, H_2O_2 reduction

currents in the hydrogen adsorption region behave the same was as O_2 reduction currents (Figure 4); *viz.*, the decrease in the peroxide reduction activity is concurrent with hydrogen adsorption. The deactivation affected by the adsorbed hydrogen is the most pronounced on Pt(111), less pronounced on Pt(100), and almost negligible on Pt(110), the same as in the case of O_2 reduction. These results imply that the deactivation by adsorbed hydrogen is entirely due to a loss of adsorption sites which break the O−O bond and not due to an interaction of O_2 with H_{ad}, as was proposed by Damjanović *et al.*[26] In fact, the activity of the Pt(111) surface was essentially nil, consistent with the quantitative two-electron reduction of O_2 in this potential region.

The structural sensitivity of O_2 and H_2O_2 reduction in the hydrogen region might be understood in terms of the state of adsorbed hydrogen on different single-crystal surfaces. Unfortunately, relatively little is known about the nature of adsorbed hydrogen on platinum in electrolytic solutions or how the adsorption sites might differ between the different surfaces. Recent *in-situ* IR data[21] suggest that hydrogen on Pt(100) is singly coordinated and possesses special optical properties, similar to those of a metal. Ogasawara and Ito[27] suggested that their IR data for hydrogen Pt(100) might be attributed to the adsorption of hydrogen in the hollow sites. Using *in-situ* X-ray scattering measurements of lattice expansion, Tidswell *et al.*[13] suggested that the 4-fold hollow sites on a Pt(100) surface are conducive to the formation of subsurface hydrogen, while the close-packed geometry of the (111) surface is not.[28] On the basis of these limited data, one might conclude that on an ideal Pt(100) surface at least part of the hydrogen lies below the surface and therefore does not significantly affect top sites, such as the a-top and bridge sites that may serve as the sites of O−O bond breaking. The IR spectra for Pt(111) show that hydrogen adsorption on Pt(111) is quite different from Pt(100), since there are no marked reflectance changes associated with hydrogen adsorption[21] nor any absorption by the terminal hydrogens.[27] Because of technical limitations, the spectral region of the multicoordinated state (500−600 cm^{-1}) of adsorbed hydrogen is difficult to study and presently remains undetected by IR. Although unidentified, it is reasonable to postulate that hydrogen on Pt(111) is a covalently bonded adsorbate sitting between surface atoms in bridge sites or 3-fold hollow sites which are also the sites where oxygen is adsorbed in UHV.[29] The nature of hydrogen on Pt(110) is even more uncertain. We can only speculate that in the case of Pt(110) the absence of an effect of the adsorbed hydrogen might be attributed to the adsorption of all of the hydrogen in the "troughs" of the surface as was proposed based on both UHV[30] and *in-situ* infrared reflection absorption spectroscopy[27] data, leaving the top-sites available for the interaction with O_2 or H_2O_2.

Acknowledgment. We thank Lee Johnson and Frank Zucca for their invaluable help in polishing the single crystals and setting up of the experimental apparatus. This work was supported by the Assistant Secretary for Conservation and Renewable Energy, Office of Transportation Technologies, Electric and Hybrid Propulsion Division of the U.S. Department of Energy, under Contract DE-AC03-76SF00098.

References and Notes

(1) Tarasevich, M. R.; Sadkowski, A.; Yeager, E. In *Kinetics and Mechanisms of Electrode Processes*; Conway, B. E., Bockris, J. O'M., Yeager, E., Khan, S. U. M., White, R. E., Eds.; Comprehensive Treatise of Electrochemistry; Plenum Press: New York, 1983; Vol. 7, pp 301−398.

(2) Kinoshita, K. *Electrochemical Oxygen Technology*; John Wiley & Sons: New York, 1992.

(3) Ross, P. N., Jr. *J. Electrochem. Soc.* **1979**, *126*, 78.

(4) Marković, N. M.; Adzić, R. R.; Cahan, B. D.; Yeager, E. B. *ISE Proceedings*; Montreaux, 1991; p 138.

(5) Marković, N. M.; Adzić, R. R.; Cahan, B. D.; Yeager, E. B. *J. Electroanal. Chem.* **1994**, *377*, 249.

(6) El Kadiri, F.; Faure, R.; Durand, R. *J. Electroanal. Chem.* **1991**, *301*, 177.

(7) Gasteiger, H. A.; Marković, N. M.; Ross, P. N., Jr. *J. Phys. Chem.*, in press.

(8) Marković, N. M.; Gasteiger, H. A.; Lucas, C.; Tidswell, I. M.; Ross, P. N., Jr. *Surf. Sci.*, in press.

(9) Brisard, G. M.; Zenati, E.; Gasteiger, H. A.; Marković, N. M.; Ross, P. N., Jr. *Langmuir*, in press.

(10) Pine Instrument Company, 101 Industrial Drive, Grove City, PA 16127.

(11) Albery, W. J.; Hitchman, M. L. *Ring-Disc Electrodes*; Oxford University Press: New York, 1971.

(12) Marković, N.; Hanson, M.; McDougal, G.; Yeager, E. *J. Electroanal. Chem.* **1986**, *241*, 309.

(13) Tidswell, I. M.; Marković, N. M.; Ross, P. N., Jr. *Phys. Rev. Lett.* **1993**, *71*, 1601.

(14) *CRC Handbook of Chemistry and Physics*, 66th ed.; Weast, R. C., Ed.; CRC Press: Boca Raton, FL, 1986.

(15) Schumpe, A.; Adler, I.; Deckwer, W.-D. *Biotechnol. Bioeng.* **1978**, *20*, 145.

(16) Anastasijević, N. A.; Dimitrijević, Z. M.; Adzić, R. R. *Electrochim. Acta* **1986**, *31*, 1125.

(17) Faguy, P. W.; Marković, N.; Adzić, R. R.; Fierro, C. A.; Yeager, E. B. *J. Electroanal. Chem.* **1990**, *289*, 245.

(18) Wieckowski, A.; Zelenay, P.; Varga, K. *J. Chim. Phys.* **1991**, *88*, 1247.

(19) Gamboa-Aldeco, M. E.; Herrero, E.; Zelenay, P. S.; Wieckowski, A. *J. Electroanal. Chem.* **1993**, *348*, 451.

(20) Faguy, P. W.; Marković, N.; Ross, P. N., Jr. *J. Electrochem. Soc.* **1993**, *140*, 1638.

(21) Nichols, R. J. In *Adsorption of Molecules at Metal Electrodes*; Lipkowski, J., Ross, P. N., Jr., Ed.; Frontiers of Electrochemistry; VCH Publishers: New York, 1992; pp 347−389.

(22) Gasteiger, H. A.; Marković, N. M.; Ross, P. N., Jr. Submitted to *J. Phys. Chem.*

(23) Zinola, C. F.; Castro Luna, A. M.; Triaca, W. E.; Arvia, A. J. *Electrochim. Acta* **1994**, *39*, 1627.

(24) Marković, N. M.; Tripković, A. V.; Marinković, N. S.; Adzić, R. R. In *Electrochemical Surface Science. Molecular Phenomena at Electrode Surfaces*; Soriaga, M. P., Ed.; ACS Symposium *Series*; Americal Chemical Society: Washington, DC, 1988; pp 497−517.

(25) Ross, P. N., Jr. *J. Chim. Phys.* **1991**, *88*, 1353.

(26) Damjanović, A.; Genshaw, M.; Bockris, J. O.'M. *J. Electrochem. Soc.* **1967**, *114*, 466.

(27) Ogasawara, H.; Ito, M. *Chem. Phys. Lett.* **1994**, *221*, 213.

(28) Tidswell, I.; Markovic, N.; Ross, P. *J. Electroanal. Chem.* **1994**, *376*, 119.

(29) Mortensen, K.; Klink, C.; Jensen, F.; Besenbacher, F.; Stensgaard, I. *Surf. Sci.* **1989**, *220*, L701.

(30) Kirsten, E.; Parschau, G.; Stocker, W.; Rieder, K. H. *Surf. Sci. Lett.* **1990**, *231*, L183.

JP942659V